Chapter 20

Central Schemes: A Powerful Black-Box Solver for Nonlinear Hyperbolic PDEs

A. Kurganov
Tulane University, New Orleans, LA, United States

Chapter Outline

ABSTRACT
We review a class of Godunov-type finite-volume methods for hyperbolic systems of conservation and balance laws—nonoscillatory central schemes. These schemes date back to 1950s, when the first-order Lax–Friedrichs scheme was introduced. The central Lax–Friedrichs scheme can be viewed as a simple alternative to the upwind Godunov scheme, which was also introduced in the 1950s. The main idea in the construction of both central and upwind first-order schemes is the same: use a global piecewise constant approximation of the solution at a certain time level and evolve it in time to the next time level exactly. The exact evolution is performed using the integral form of the studied system of PDEs. The difference is in one small detail—which is in fact not small at all—how to select the space–time control volume for the time evolution. The key idea in the construction of central schemes is to choose these control volume in such a way that no (localized) Riemann problems need to be solved at the evolution step. This makes central schemes particularly simple and universal numerical tool for general hyperbolic systems. On the other hand, central schemes are based on averaging the nonlinear waves rather than resolving them and thus they have larger numerical

Handbook of Numerical Analysis, Vol. 17. http://dx.doi.org/10.1016/bs.hna.2016.09.008

dissipation than their upwind counterparts. In order to increase the resolution achieved by central schemes, one has to increase their order. We describe how to design high-order nonoscillatory central schemes and also discuss how to further decrease their numerical dissipation without risking oscillations. The latter is achieved by utilizing some upwinding information (local speeds of propagation) within the framework of the Riemann-problem-solver-free central schemes and modifying the set of control volumes used for the time evolution. This leads to another type of central schemes—central-upwind schemes, whose derivation is reviewed in this work.

AMS Classification Codes: 65M08, 76M12, 35L65

Keywords: Hyperbolic systems of conservation and balance laws, Godunov-type finite-volume methods, Staggered central schemes, Central-upwind schemes, Piecewise polynomial reconstruction

1 A VERY BRIEF THEORETICAL BACKGROUND

We consider one-dimensional (1D) hyperbolic systems of conservation laws,

$$\boldsymbol{q}_t + \boldsymbol{f}(\boldsymbol{q})_x = \boldsymbol{0}, \tag{1}$$

subject to the prescribed initial data

$$\boldsymbol{q}(x,0) = \boldsymbol{q}_0(x). \tag{2}$$

Here, x is a space variable, t is time, $\boldsymbol{q} = \boldsymbol{q}(x, t)$ is a vector of unknown quantities in $\mathbb{R}^N$, $\boldsymbol{f}(\boldsymbol{q})$ is the flux vector.

It is well known that solutions of the initial value problems (IVPs) (1), (2) do not necessarily preserve their initial smoothness. Moreover, even when the initial data are infinitely smooth, solutions of these IVPs may break down and develop such nonsmooth structures as shock waves, contact discontinuities, rarefaction waves and even singular δ-shocks. In such a generic case, the nonsmooth solutions are nonclassical (weak) and they are to be understood in the sense of distributions. Namely, we say that $\boldsymbol{q}$ is a weak solution of the IVP (1), (2), if it satisfies the weak formulation of (1), (2),

$$\int_0^\infty\int_{\mathbb{R}} [\boldsymbol{q}(x,t)\varphi_x(x,t) + \boldsymbol{f}(\boldsymbol{q}(x,t))\varphi_t(x,t)]dx\,dt + \int_{\mathbb{R}} \boldsymbol{q}(x,0)\varphi(x,0)\,dx = 0,$$

for any smooth and compactly supported test function φ with supp $\varphi \subset \mathbb{R}\times[0,\infty)$. Weak solutions, however, are not unique and to single out the unique physically relevant solution, one needs to require the weak solution either to be the limit of the vanishing viscosity approximation of the studied hyperbolic system or satisfy a certain additional criterion such as an entropy condition. For this and other analytical results on nonlinear hyperbolic partial differential equations

(PDEs), we refer the reader, e.g., to Dafermos (2010), LeFloch (2002), Li et al. (1998), Serre (1999), Smoller (1994) and Zheng (2001).

2 FINITE-VOLUME FRAMEWORK

Finite-volume methods are based on the integral form of the system (1), which we integrate over a space–time control volume $[a, b] \times [c, d]$ to obtain the following system of integral equations:

$$\int_a^b \boldsymbol{q}(x,d)\,dx = \int_a^b \boldsymbol{q}(x,c)\,dx - \int_c^d [\boldsymbol{f}(\boldsymbol{q}(b,t)) - \boldsymbol{f}(\boldsymbol{q}(a,t))]dt. \tag{3}$$

If these equations are satisfied for any $a < b$ and $0 \le c \le d$, then the systems (1) and (3) are equivalent for piecewise smooth weak solutions. Therefore, Eq. (3) can be considered as a definition of a weak piecewise smooth solution, and we would like to point out that only piecewise smooth solutions—not general weak solutions—can be computed numerically.

In order to design a numerical method based on the integral equations (3), we will first introduce small scales in both space (Δx) and time (Δt) and take the space–time control volume to be $\left[x - \frac{\Delta x}{2}, x + \frac{\Delta x}{2}\right] \times [t, t + \Delta t]$, for which equation (3) after the division by Δx reads as

$$\bar{\boldsymbol{q}}(x,t+\Delta t) = \bar{\boldsymbol{q}}(x,t) - \lambda\left[\hat{\boldsymbol{f}}\left(x+\frac{\Delta x}{2},t\right) - \hat{\boldsymbol{f}}\left(x-\frac{\Delta x}{2},t\right)\right], \tag{4}$$

where $\lambda := \dfrac{\Delta t}{\Delta x}$,

$$\bar{\boldsymbol{q}}(x,t) := \frac{1}{\Delta x}\int_{x-\frac{\Delta x}{2}}^{x+\frac{\Delta x}{2}} \boldsymbol{q}(\xi,t)\,d\xi \tag{5}$$

is a so-called sliding average of $\boldsymbol{q}$, and

$$\hat{\boldsymbol{f}}(x,t) := \frac{1}{\Delta t}\int_t^{t+\Delta t} \boldsymbol{f}(\boldsymbol{q}(x,\tau))\,d\tau \tag{6}$$

is the averaged flux across x during the time interval $[t, t + \Delta t]$.

Formula (4) serves as a starting point of finite-volume evolution, which is performed in the following three steps. First, the computational domain is split into nonoverlapping intervals (in fact, one may also consider overlapping intervals as it was done in, e.g., Liu (2005), Liu et al. (2007), Liu et al. (2009)

and Yang et al. (2015)). Then, if a (global in space) approximate solution is available at time level t, one may use the definition of a sliding average (5) to compute $\bar{\boldsymbol{q}}(x,t)$ at the centers of the selected intervals. Finally, one should evaluate the averaged fluxes (6) to obtain the set of the sliding averages $\bar{\boldsymbol{q}}(x,t+\Delta t)$ at the same points in space. Finite-volume evolution via an arbitrary set of space–time control volumes is schematically shown in the (x, t)-plane in Fig. 1.

Since the data obtained at the end of each finite-volume evolution step will consist of the sliding averages computed at a certain set of points, construction of a finite-volume method should begin with selection of grid intervals, which we denote by $C_j := (x_{j-\frac{1}{2}}, x_{j+\frac{1}{2}})$. For the sake of simplicity, let us assume that the mesh is uniform, that is, $x_{j+\frac{1}{2}} - x_{j-\frac{1}{2}} = \Delta x$ for all j and the cell centers are $x_j = x_{j-\frac{1}{2}} + \Delta x/2$. We now assume that the sliding averages over the grid cells are available at time level t^n. These sliding averages are called the cell averages and denoted by

$$\bar{\boldsymbol{q}}_j^{\,n} := \frac{1}{\Delta x}\int_{C_j} \boldsymbol{q}(x,t^n)\,dx.$$

Equipped with the given set of cell averages, one can easily obtain a global piecewise constant approximation of the solution:

$$\tilde{\boldsymbol{q}}^n(x) := \sum_j \bar{\boldsymbol{q}}_j^{\,n}\chi_{C_j}, \tag{7}$$

where χ_{C_j} is the characteristic function of the interval C_j. We now can complete the finite-volume evolution step, but the way the averaged fluxes,

$$\hat{\boldsymbol{f}}(x,t^n) := \frac{1}{\Delta t^n}\int_{t^n}^{t^{n+1}} \boldsymbol{f}(\boldsymbol{q}(x,t))\,dt, \quad t^{n+1} := t^n + \Delta t^n, \tag{8}$$

are computed depends on the way the space–time control volumes are selected. This is a crucial point in the construction of finite-volume methods.

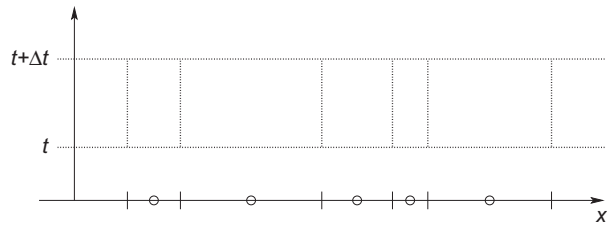

FIG. 1 Space–time control volumes. *Circles* "∘" represent the centers of space intervals.

There are two major approaches, which lead to two different classes of schemes—upwind and central ones.

Remark 1. We note that the piecewise constant approximation (7) is only first-order accurate. In order to increase the order of accuracy, one needs to use higher-order interpolants instead of (7), as discussed in Section 5.

3 FIRST-ORDER UPWIND SCHEMES

The first finite-volume upwind scheme is the Godunov scheme proposed in Godunov (1959). The importance of this work is recognized in the fact that finite-volume methods are often called Godunov-type schemes.

In the upwind setting, the finite-volume evolution is carried out using the space–time control volumes $\left[x_{j-\frac{1}{2}}, x_{j+\frac{1}{2}}\right] \times [t^n, t^{n+1}]$ outlined in Fig. 2 (left). This means that, in fact, one simply needs to substitute the values $x = x_j$ and $t = t^n$ into (4) to obtain

$$\bar{\boldsymbol{q}}_j^{\,n+1} = \bar{\boldsymbol{q}}_j^{\,n} - \lambda\left[\hat{\boldsymbol{f}}\left(x_{j+\frac{1}{2}}, t^n\right) - \hat{\boldsymbol{f}}\left(x_{j-\frac{1}{2}}, t^n\right)\right], \tag{9}$$

and thus, in order to complete the construction of the scheme one has to evaluate the averaged fluxes

$$\hat{\boldsymbol{f}}\left(x_{j+\frac{1}{2}}, t^n\right) = \frac{1}{\Delta t^n}\int\limits_{t^n}^{t^{n+1}} \boldsymbol{f}\left(\boldsymbol{q}\left(x_{j+\frac{1}{2}}, t\right)\right) dt. \tag{10}$$

After the integrals in (10) are (approximately) evaluated, one obtains the corresponding numerical fluxes denoted by $\boldsymbol{H}^n_{j+\frac{1}{2}} \approx \hat{\boldsymbol{f}}\left(x_{j+\frac{1}{2}}, t^n\right)$, and the resulting upwind scheme can be written as

$$\bar{\boldsymbol{q}}_j^{\,n+1} = \bar{\boldsymbol{q}}_j^{\,n} - \lambda^n\left[\boldsymbol{H}^n_{j+\frac{1}{2}} - \boldsymbol{H}^n_{j-\frac{1}{2}}\right], \quad \lambda^n := \frac{\Delta t^n}{\Delta x}. \tag{11}$$

In the classical Godunov scheme, the integrals in (10) are evaluated exactly. This is possible thanks to the one of the most important properties

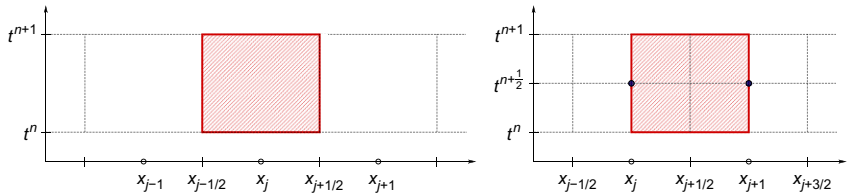

FIG. 2 Space–time control volumes: upwind (*left*) and central (*right*) settings.

of hyperbolic systems—finite speed of propagation, which is determined by the largest spectral radius of the Jacobian $A(\boldsymbol{q}) := \partial \boldsymbol{f}/\partial \boldsymbol{q}$ calculated over the entire computational domain at time $t = t^n$. Namely, the waves generated at the cell interfaces $x = x_{j+\frac{1}{2}}$ at time $t = t^n$, at which the approximate solution is a piecewise constant function $\boldsymbol{q}(x, t^n) = \hat{\boldsymbol{q}}^n(x)$, will not propagate faster than with the speed

$$a^n := \max_j \left\{ \rho\left(A(\bar{\boldsymbol{q}}_j^n) \right) \right\}, \tag{12}$$

where $\rho(A)$ is a spectral radius of the matrix A. Therefore, if the time step is restricted by

$$\Delta t^n \le \frac{\Delta x}{a^n}, \tag{13}$$

the solution $\boldsymbol{q}\left(x_{j+\frac{1}{2}}, t\right)$ at the time interval $[t^n, t^{n+1}]$ needed to evaluate the time integral in (10) will not be affected by the (nonlinear) waves generated at other cell interfaces. Thus, in order to compute the required values of $\boldsymbol{q}\left(x_{j+\frac{1}{2}}, t\right)$, one has to solve the following Riemann problem: the system (1) subject to the initial data

$$\boldsymbol{q}(x, t^n) = \begin{cases} \bar{\boldsymbol{q}}_j^n, & \text{if} \quad x < x_{j+\frac{1}{2}}, \\ \bar{\boldsymbol{q}}_{j+1}^n, & \text{if} \quad x > x_{j+\frac{1}{2}}, \end{cases} . \tag{14}$$

prescribed at time $t = t^n$. It is well known (see, e.g., Dafermos, 2010; LeFloch, 2002; Li et al., 1998; Serre, 1999; Smoller, 1994; Zheng, 2001) that solutions of Riemann problems for hyperbolic systems of conservation laws are self-similar and therefore the corresponding wave propagation can be schematically shown using the straight lines originating at the points $\left(x_{j+\frac{1}{2}}, t^n\right)$ in the space–time plane, see Fig. 3 (left).

Remark 2. Note that in the literature, Riemann initial data are usually prescribed at time $t = 0$ and the breaking point of the initial data is typically $x = 0$. However,

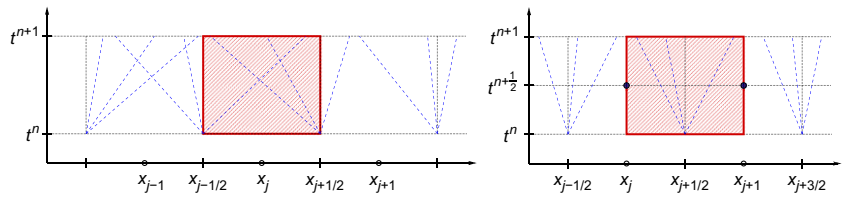

FIG. 3 Wave propagation in upwind (*left*) and central (*right*) settings. *Dashed lines* represent Riemann fans generated at each cell interface at time $t = t^n$.

due to the translation invariance of the hyperbolic systems (1), one can shift the data by $x_{j+\frac{1}{2}}$ and t^n without affecting any solution properties.

Since the self-similar solution of the Riemann problem (1), (14) is $\boldsymbol{q}(x,t)=\boldsymbol{\mathcal{R}}^{\,n}_{j+\frac{1}{2}}(\xi)$, where the self-similar coordinate is $\xi=\left(x-x_{j+\frac{1}{2}}\right)/(t-t^n)$ and $t>t^n$, the solution $\boldsymbol{q}\left(x_{j+\frac{1}{2}},t\right)=\boldsymbol{\mathcal{R}}^{\,n}_{j+\frac{1}{2}}(0)$ for all $t>t^n$ and therefore the integrals in (10) are immediately obtained. This results in the numerical flux $\boldsymbol{H}^n_{j+\frac{1}{2}}=\boldsymbol{f}\left(\boldsymbol{\mathcal{R}}^{\,n}_{j+\frac{1}{2}}(0)\right)$ and the classical Godunov scheme can be written as

$$\bar{\boldsymbol{q}}_j^{\,n+1}=\bar{\boldsymbol{q}}_j^{\,n}-\lambda^n\left[\boldsymbol{f}\left(\boldsymbol{\mathcal{R}}^{\,n}_{j+\frac{1}{2}}(0)\right)-\boldsymbol{f}\left(\boldsymbol{\mathcal{R}}^{\,n}_{j-\frac{1}{2}}(0)\right)\right]. \tag{15}$$

Unfortunately, the Godunov scheme (15) has a serious drawback: it relies on the exact solution of the Riemann problem, which may be computationally expensive and very hard (or even impossible) to obtain analytically. The major difficulty in solving Riemann problems exactly is a very complicated structure of their solutions. Indeed, for the $N\times N$ system (1) the solution of the Riemann problem, in general, consists of N waves, which are not easy to compute analytically.

Since 1960s many approximate Riemann problem solvers have been designed as alternatives to the exact one used in (15). One of the possible strategies in constructing approximate solvers is to replace the exact wave structure with the approximate one. For instance, taking into account the fastest waves only, one obtains the Rusanov scheme (see Rusanov, 1961), which can be written in the form (11) with the following numerical flux:

$$\boldsymbol{H}^n_{j+\frac{1}{2}}=\frac{1}{2}\left[\boldsymbol{f}(\bar{\boldsymbol{q}}^{\,n}_{j+1})+\boldsymbol{f}(\bar{\boldsymbol{q}}_j^{\,n})\right]-\frac{a^n_{j+\frac{1}{2}}}{2}\left[\bar{\boldsymbol{q}}^{\,n}_{j+1}-\bar{\boldsymbol{q}}_j^{\,n}\right], \tag{16}$$

where $a^n_{j+\frac{1}{2}}$ are the local propagation speeds, computed using the spectral radius of the Jacobian as follows:

$$a^n_{j+\frac{1}{2}}=\max\left\{\rho\left(A(\bar{\boldsymbol{q}}^{\,n}_{j+1})\right),\rho\left(A(\bar{\boldsymbol{q}}_j^{\,n})\right)\right\}. \tag{17}$$

Considering both fastest left- and right-going waves results in a more accurate approximate Riemann problem solver, which leads to the Harten–Lax–van Leer (HLL) scheme (see Harten et al., 1983), which can also be put into the same form (11), but with a different numerical flux:

$$\boldsymbol{H}^n_{j+\frac{1}{2}}=\frac{a^{n+}_{j+\frac{1}{2}}\boldsymbol{f}(\bar{\boldsymbol{q}}_j^{\,n})-a^{n-}_{j+\frac{1}{2}}\boldsymbol{f}(\bar{\boldsymbol{q}}^{\,n}_{j+1})}{a^{n+}_{j+\frac{1}{2}}-a^{n-}_{j+\frac{1}{2}}}+\frac{a^{n+}_{j+\frac{1}{2}}a^{n-}_{j+\frac{1}{2}}}{a^{n+}_{j+\frac{1}{2}}-a^{n-}_{j+\frac{1}{2}}}\left[\bar{\boldsymbol{q}}^{\,n}_{j+1}-\bar{\boldsymbol{q}}_j^{\,n}\right], \tag{18}$$

where $a^{n\pm}_{j+\frac{1}{2}}$ are the one-sided local propagation speeds, computed using the largest and smallest eigenvalues of the Jacobian as follows:

$$a^{n+}_{j+\frac{1}{2}} = \max\left\{\lambda_N\left(A(\bar{\boldsymbol{q}}^{\,n}_{j+1})\right), \lambda_N\left(A(\bar{\boldsymbol{q}}^{\,n}_{j})\right), 0\right\}, \quad a^{n-}_{j+\frac{1}{2}} = \min\left\{\lambda_1\left(A(\bar{\boldsymbol{q}}^{\,n}_{j+1})\right), \lambda_1\left(A(\bar{\boldsymbol{q}}^{\,n}_{j})\right), 0\right\}. \tag{19}$$

Here, $\lambda_1(A) \le \cdots \le \lambda_N(A)$ denote the ordered set of the eigenvalues of the matrix A. The HLL scheme was further improved by taking into account of the presence of slower (linear) contact waves in Einfeld (1988) and Toro et al. (1994), where modified HLL schemes were developed.

Remark 3. We note that both Rusanov and HLL schemes are, in fact, central schemes; see Remark 13.

An alternative approach for designing approximate Riemann problem solvers was proposed by Roe in 1981. The idea is to locally replace a complicated nonlinear hyperbolic system with a linear one, namely, to evaluate the numerical flux at $x = x_{j+\frac{1}{2}}$ by solving a linearized system with constant coefficients

$$\boldsymbol{q}_t + A^n_{j+\frac{1}{2}} \boldsymbol{q}_x = \boldsymbol{0}, \tag{20}$$

subject to the same initial data (14). Here, $A^n_{j+\frac{1}{2}}$ is a proper linearization of the Jacobian $A(\boldsymbol{q})$. The classical Roe scheme is obtained by constructing the Roe matrix $\hat{\boldsymbol{A}}^n_{j+\frac{1}{2}}$ satisfying the condition $\boldsymbol{f}(\bar{\boldsymbol{q}}^{\,n}_{j+1}) - \boldsymbol{f}(\bar{\boldsymbol{q}}^{\,n}_{j}) = \hat{\boldsymbol{A}}^n_{j+\frac{1}{2}}(\bar{\boldsymbol{q}}^{\,n}_{j+1} - \bar{\boldsymbol{q}}^{\,n}_{j})$, which guarantees that if the states $\bar{\boldsymbol{q}}^{\,n}_{j}$ and $\bar{\boldsymbol{q}}^{\,n}_{j+1}$ correspond to an isolated shock wave, its speed will coincide with the speed of the linearized wave, and taking $A^n_{j+\frac{1}{2}} = \hat{\boldsymbol{A}}^n_{j+\frac{1}{2}}$ in (20). For some systems, however, it is not easy to construct the Roe matrix. A much simpler approach was advocated in Buffard et al. (2000), Gallouët et al. (2002) and Masella et al. (1999), where the so-called VFRoe scheme was developed by simply taking $A^n_{j+\frac{1}{2}} = A(\boldsymbol{q}_{j+\frac{1}{2}})$, where $\boldsymbol{q}_{j+\frac{1}{2}} := \frac{1}{2}(\bar{\boldsymbol{q}}^{\,n}_{j+1} + \bar{\boldsymbol{q}}^{\,n}_{j})$.

For both the Roe and VFRoe schemes, the solution of the IVP (20) and (14) is self-similar and easy to obtain by diagonalizing the system (20) using the characteristic variables. We denote this solution by $\boldsymbol{q}(x,t) = \mathcal{L}^n_{j+\frac{1}{2}}(\xi)$ so that the numerical flux in (11) reduces to $\boldsymbol{H}^n_{j+\frac{1}{2}} = \boldsymbol{f}\left(\mathcal{L}^{\,n}_{j+\frac{1}{2}}(0)\right)$, and the resulting scheme reads as

$$\bar{\boldsymbol{q}}^{\,n+1}_{j} = \bar{\boldsymbol{q}}^{\,n}_{j} - \lambda^n\left[\boldsymbol{f}\left(\mathcal{L}^{\,n}_{j+\frac{1}{2}}(0)\right) - \boldsymbol{f}\left(\mathcal{L}^{\,n}_{j-\frac{1}{2}}(0)\right)\right]. \tag{21}$$

For a detailed description and derivation of the aforementioned and other popular approximate Riemann problem solvers as well as for their comparative study, we refer the reader to Toro (2009); see also Godlewski and Raviart (1996), Kröner (1997) and LeVeque (2002).

4 FIRST-ORDER CENTRAL SCHEMES

Central schemes can be considered as a simple Riemann-problem-solver-free alternative to upwind schemes. Unfortunately, a straightforward central-difference approximation of the space derivatives in (1) leads to the finite-difference scheme

$$\boldsymbol{q}_j^{n+1} = \boldsymbol{q}_j^n - \frac{\lambda^n}{2}\left[\boldsymbol{f}(\boldsymbol{q}_{j+1}^n) - \boldsymbol{f}(\boldsymbol{q}_{j-1}^n)\right], \tag{22}$$

which is known to be unconditionally unstable and thus prone to uncontrolled oscillations. In 1954, Lax (1954) and Friedrichs (1954) proposed a stabilized version of the scheme (22)—the celebrated Lax–Friedrichs scheme:

$$\boldsymbol{q}_j^{n+1} = \frac{\boldsymbol{q}_{j+1}^n + \boldsymbol{q}_{j-1}^n}{2} - \frac{\lambda^n}{2}\left[\boldsymbol{f}(\boldsymbol{q}_{j+1}^n) - \boldsymbol{f}(\boldsymbol{q}_{j-1}^n)\right]. \tag{23}$$

Note that in both (22) and (23), the evolved quantities are the point values of $\boldsymbol{q}$ at the grid nodes rather than the cell averages. Even though these schemes can be artificially put into the finite-volume form (11) with appropriate fluxes, they are not Godunov-type schemes in the sense that they cannot be rigorously derived using the finite-volume framework described in Section 2.

The first-order Godunov-type central scheme is obtained using exactly the same finite-volume evolution equations (4)–(6), which were used to design upwind schemes in Section 3, but sampled at a different set of points: $\left(x_{j+\frac{1}{2}}, t^n\right)$ instead of (x_j, t^n), as illustrated in Fig. 2. Compared to the upwind setting, the space–time control volumes $[x_j, x_{j+1}] \times [t^n, t^{n+1}]$ used in the construction of central schemes, is shifted by $\Delta x/2$, see Fig. 2 (right).

We stress that while the data at time level $t = t^n$ is given over the original grid $\left[x_{j-\frac{1}{2}}, x_{j+\frac{1}{2}}\right]$, the new computed solution will be realized over the staggered grid. Indeed, Eqs. (4)–(6) will now lead to

$$\bar{\boldsymbol{q}}_{j+\frac{1}{2}}^{n+1} = \frac{1}{\Delta x}\int_{x_j}^{x_{j+1}} \tilde{\boldsymbol{q}}^n(x)\,dx - \frac{\lambda^n}{\Delta t^n}\int_{t^n}^{t^{n+1}} \left[\boldsymbol{f}(\boldsymbol{q}(x_{j+1},t)) - \boldsymbol{f}(\boldsymbol{q}(x_j,t))\right]dt. \tag{24}$$

The space integral on the right-hand side (RHS) of (24) is just an integral of a piecewise constant function (7) and thus can be exactly evaluated in a straightforward manner. The time integrals on the RHS of (24) are not easy to compute unless the timestep restriction is tightened and Δt^n is taken to be twice smaller compared to (13), namely,

$$\Delta t^n \le \frac{\Delta x}{2a^n}. \tag{25}$$

As one can see in Fig. 3 (right), no waves generated at the cell interfaces can reach the vertical segments at $x = x_j$ for $t \in [t^n, t^{n+1}]$, and thus the solution of

the system (1) subject to the piecewise constant initial data $\boldsymbol{q}(x,t^n)=\widetilde{\boldsymbol{q}}^{\,n}(x)$ remains constant there. Therefore, after evaluating all of the integrals in (24), we obtain the first-order staggered central scheme—staggered Lax–Friedrichs scheme (see Nessyahu and Tadmor, 1990):

$$\bar{\boldsymbol{q}}_{j+\frac{1}{2}}^{\,n+1}=\frac{\bar{\boldsymbol{q}}_{j+1}^{\,n}+\bar{\boldsymbol{q}}_{j}^{\,n}}{2}-\lambda^n\left[\boldsymbol{f}(\bar{\boldsymbol{q}}_{j+1}^{\,n})-\boldsymbol{f}(\bar{\boldsymbol{q}}_{j}^{\,n})\right]. \tag{26}$$

Central schemes (both Lax–Friedrichs and staggered Las-Friedrichs ones) are extremely simple and universal tool for solving hyperbolic systems of conservation laws. They, however, have a substantial disadvantage compared to the upwind schemes—their numerical viscosity is much larger (see, e.g., Tadmor, 1984a,b), which leads to excessive smearing of discontinuous and other "rough" parts of the computed solution. In fact, first-order upwind schemes are also quite diffusive and cannot provide high resolution of non-smooth parts of the solution (especially of linear contact waves) unless very small Δx and Δt^n are used and the latter may be computationally unaffordable. The way to enhance the resolution is to increase the order of the scheme.

5 HIGH-ORDER FINITE-VOLUME METHODS

We first note that both the Godunov (15) and staggered Lax–Friedrichs (26) schemes are based on the exact finite-volume evolution of the computed solution. Therefore, the loss of accuracy occurs at the approximation step, when the global first-order accurate piecewise constant interpolant (7) is reconstructed from the set of computed cell averages. In order to increase the (formal) order of accuracy of the approximation and thus of the entire scheme, one should replace the piecewise constant approximation with a higher-order one.

5.1 Second-Order Upwind Schemes

The first second-order Godunov-type scheme was introduced by van Leer in 1979, where the so-called MUSCL approach was proposed. It is based on a piecewise linear reconstruction

$$\widetilde{\boldsymbol{q}}^{\,n}(x):=\sum_j\left[\bar{\boldsymbol{q}}_j^{\,n}+(\boldsymbol{q}_x)_j^n(x-x_j)\right]\chi_{C_j}, \tag{27}$$

which will be second-order accurate provided the slopes $(\boldsymbol{q}_x)_j^n\approx\boldsymbol{q}_x(x_j,t^n)$ within at least first order of accuracy. To keep the resulting scheme from being too oscillatory, one has to use a nonlinear limiter in the computation of $(\boldsymbol{q}_x)_j^n$ to ensure that no large over- or undershoots of size $\mathcal{O}(1)$ are created at the cell interfaces. A library of such limiters is available; we refer the reader, e.g., to Godlewski and Raviart (1996), Kröner (1997), LeVeque

(2002), Lie and Noelle (2003), Nessyahu and Tadmor (1990), Sweby (1984) and van Leer (1979). They may be applied to the vector quantity $\boldsymbol{q}$ either in a componentwise manner, that is, to each component of $\boldsymbol{q}$ directly, or using the local characteristic decompositions as it was done, for instance, in Qiu and Shu (2002). The latter approach results in the schemes that are in general less oscillatory, but more computationally expensive.

When the piecewise constant interpolant is replaced with a piecewise linear one, the finite-volume evolution procedure must be modified. It is not so easy to do in the framework of upwind schemes, since now instead of solving the Riemann problems at each cell interface, one has to solve the generalized Riemann problem: the system (1) subject to the initial data

$$\boldsymbol{q}(x,t^n)=\begin{cases}\bar{\boldsymbol{q}}_j^{\,n}+(\boldsymbol{q}_x)_j^n(x-x_j), & \text{if} \quad x<x_{j+\frac{1}{2}},\\ \bar{\boldsymbol{q}}_{j+1}^{\,n}+(\boldsymbol{q}_x)_{j+1}^n(x-x_{j+1}), & \text{if} \quad x>x_{j+\frac{1}{2}},\end{cases} \tag{28}$$

prescribed at time $t=t^n$. For certain hyperbolic systems of conservation laws the exact solution of the generalized Riemann problem can be constructed; see Ben-Artzi and Falcovitz (2003). However, these solutions are very complicated and quite computationally expensive. As an alternative, one can design an approximate generalized Riemann problem solver, see, e.g., Godlewski and Raviart (1996), Kröner (1997), LeVeque (2002) and Toro (2009).

5.2 Second-Order Nessyahu–Tadmor Scheme

Another alternative is to switch to the central framework, in which the fact that the data are now piecewise linear does not lead to any substantial increase in the level of complexity since the solution still remains smooth at the cell centers for $t\in[t^n,\,t^{n+1}]$ provided the timestep restriction (25) with

$$a^n:=\max_x\left\{\rho\left(A(\tilde{\boldsymbol{q}}^{\,n}(x))\right)\right\}$$

is satisfied. After noticing this, the second-order staggered central scheme—the Nessyahu–Tadmor scheme (Nessyahu and Tadmor, 1990)—is now designed as follows.

First, we evaluate the space integral on the RHS of (24) exactly, which is straightforward since we simply need to integrate two linear pieces:

$$\begin{aligned}\frac{1}{\Delta x}\int_{x_j}^{x_{j+1}}\tilde{\boldsymbol{q}}^{\,n}(x)\,dx&=\frac{1}{\Delta x}\left\{\int_{x_j}^{x_{j+\frac{1}{2}}}\left[\bar{\boldsymbol{q}}_j^{\,n}+(\boldsymbol{q}_x)_j^n(x-x_j)\right]dx+\int_{x_{j+\frac{1}{2}}}^{x+1}\left[\bar{\boldsymbol{q}}_{j+1}^{\,n}+(\boldsymbol{q}_x)_{j+1}^n(x-x_{j+1})\right]dx\right\}\\&=\frac{\bar{\boldsymbol{q}}_{j+1}^{\,n}+\bar{\boldsymbol{q}}_j^{\,n}}{2}+\frac{\Delta x}{8}\left[(\boldsymbol{q}_x)_j^n-(\boldsymbol{q}_x)_{j+1}^n\right].\end{aligned} \tag{29}$$

We then approximate the time integrals of the smooth functions of t on the RHS of (24) using the midpoint rule so that

$$\frac{1}{\Delta t^n}\int_{t^n}^{t^{n+1}} \boldsymbol{f}(\boldsymbol{q}(x_j,t))\,dt \approx \boldsymbol{f}\left(\boldsymbol{q}_j^{\,n+\frac{1}{2}}\right), \tag{30}$$

where the values of $\boldsymbol{q}$ at the points $(x_j, t^{n+\frac{1}{2}})$ marked by the filled circles in Figs. 2 and 3 on the right can be obtained using the Taylor expansion in t (which is valid since the solution is smooth there) in the following way:

$$\boldsymbol{q}_j^{\,n+\frac{1}{2}} = \tilde{\boldsymbol{q}}^{\,n}(x_j) + \frac{\Delta t^n}{2}\,\boldsymbol{q}_t(x_j,t^n) = \bar{\boldsymbol{q}}_j^{\,n} - \frac{\Delta t^n}{2}\boldsymbol{f}(\bar{\boldsymbol{q}}_j^{\,n})_x. \tag{31}$$

Here, the numerical derivatives $\boldsymbol{f}(\bar{\boldsymbol{q}}_j^{\,n})_x$ can be computed either using $\boldsymbol{f}(\bar{\boldsymbol{q}}_j^{\,n})_x = A(\bar{\boldsymbol{q}}_j^{\,n})(\boldsymbol{q}_x)_j^n$, or by applying the same limiter used in computing the slopes in (27) to the set of the flux values $\boldsymbol{f}(\boldsymbol{q}_{\mathbf{j}}^{\mathbf{n}})$. Finally, we substitute (29)–(31) into (24) and obtain the Nessyahu–Tadmor scheme:

$$\bar{\boldsymbol{q}}_{j+\frac{1}{2}}^{\,n+1} = \frac{\bar{\boldsymbol{q}}_{j+1}^{\,n} + \bar{\boldsymbol{q}}_j^{\,n}}{2} + \frac{\Delta x}{8}\left[(\boldsymbol{q}_x)_j^n - (\boldsymbol{q}_x)_{j+1}^n\right] - \lambda^n\left[\boldsymbol{f}\left(\boldsymbol{q}_{j+1}^{\,n+\frac{1}{2}}\right) - \boldsymbol{f}\left(\boldsymbol{q}_j^{\,n+\frac{1}{2}}\right)\right]. \tag{32}$$

Remark 4. One can view the Nessyahu–Tadmor scheme as a predictor–corrector method, in which (31) is a first-order predictor and (32) is the second-order corrector.

Remark 5. Staggered central schemes have been extended to the case of multiple space dimensions both on Cartesian (Jiang and Tadmor, 1998) and unstructured (Arminjon et al., 1997) grids.

5.3 High-Order Schemes

In order to further increase the order of the finite-volume methods, one needs to further increase the accuracy of the piecewise polynomial reconstruction. Third-order schemes can be constructed using piecewise parabolic interpolants $\tilde{\boldsymbol{q}}^{\,n}(x)$. It should be pointed out though that it is much harder to ensure nonoscillatory properties of higher than second order piecewise polynomials. For instance, several third-order piecewise parabolic reconstructions satisfying the number of extrema nonincreasing property were introduced in Kurganov and Petrova (2001), Liu and Osher (1996) and Liu and Tadmor (1998). An alternative approach of constructing high-order essentially nonoscillatory interpolant is based on the idea of differentiating in the direction of smoothness, which was realized in so-called ENO reconstructions; see, e.g., Abgrall (1994), Cockburn et al. (1998) and Harten et al. (1987). Other popular high-order reconstructions are based on the idea of taking a linear combinations of several polynomial pieces (each of which is obtained by differentiating in different directions) with

the weights inversely proportional to the their smoothness measured in Sobolev spaces. This leads to a class of weighted ENO (WENO) schemes; see, e.g., Cockburn et al. (1998), Jiang and Shu (1996), Shi et al. (2002), Shu (2003) and Shu (2009). Unlike their counterparts, WENO reconstructions employ polynomials of lower degree and thus they are not uniformly high-order—only the data needed for evolving solutions in time (point values of the solution at the cell interfaces) are computed within the desired high accuracy. Therefore, when applied in the staggered central framework, WENO reconstructions have to be modified to accurately approximate the integrals $\int_{x_j}^{x_{j+\frac{1}{2}}} \widetilde{\boldsymbol{q}}^{\,n}(x)\,dx$ and $\int_{x_{j+\frac{1}{2}}}^{x_{j+1}} \widetilde{\boldsymbol{q}}^{\,n}(x)\,dx$. This was achieved in Bianco et al. (1999), Levy et al. (1999), Levy et al. (2000) and Levy et al. (2002), where a class of central WENO (CWENO) schemes was introduced.

Remark 6. For finite-volume methods of higher than second order, reconstruction procedures based on nonlinear limiters are typically computationally expensive. One can alternatively enforce stability by adding an artificial viscosity and not using any limiters. This idea was first proposed in 1950 in von Neumann and Richtmyer (1950) and since then it was notably adopted in many works including Caramana et al. (1998), Shchepetkin and McWilliams (1998), Wilkins (1980) and among others. One, however, has to be careful since adding artificial viscosity terms may cause either the discontinuities to be oversmeared or the oscillations not to be sufficiently damped. Highly accurate and robust artificial viscosity methods with the viscosity coefficients being proportional to either the weak local residual (Kurganov and Liu, 2012) or entropy production (Guermond and Pasquetti, 2008; Guermond et al., 2011) have been recently proposed.

6 CENTRAL-UPWIND SCHEMES

Even though the use of higher-order reconstructions significantly improves the resolution achieved by both upwind and staggered central schemes, central schemes may suffer from excessive numerical viscosity, which is of order $\mathcal{O}((\Delta x)^{2r}/\Delta t^n)$, where r is the formal order of the scheme. In order to illustrate this point, we rewrite the simplest staggered central scheme—the first-order Lax–Friedrichs scheme—in the following equivalent form:

$$\frac{\boldsymbol{q}^{n+1}_{j+\frac{1}{2}}-\boldsymbol{q}^{n}_{j+\frac{1}{2}}}{\Delta t^n}+\frac{\boldsymbol{f}(\boldsymbol{q}^n_{j+1})-\boldsymbol{f}(\boldsymbol{q}^n_j)}{\Delta x}=\frac{(\Delta x)^2}{8\Delta t^n}\cdot\frac{\boldsymbol{q}^n_{j+1}-2\boldsymbol{q}^n_{j+\frac{1}{2}}+\boldsymbol{q}^n_j}{(\Delta x/2)^2}. \tag{33}$$

Note that here we have replaced the cell averages of $\boldsymbol{q}$ in (26) with the corresponding point values (this can be done since for both first- and second-order schemes, these quantities are equal). The terms on the left-hand side

(LHS) of (33) clearly approximate the corresponding terms on the LHS of (1) and the term on the RHS of (33) represents the numerical viscosity with the viscosity coefficient being $\mathcal{O}((\Delta x)^2/\Delta t^n)$.

Therefore, numerical viscosity present in staggered central schemes is particularly large when sufficiently small timesteps are enforced, for instance, due to the presence of (degenerate) diffusion and/or source terms, or if the final computational time is very large as it may be the case when steady-state solutions are to be captured. One can reduce the numerical dissipation by modifying the central finite-volume evolution procedure. This leads to a new class of Godunov-type Riemann-problem-solver-free central schemes—central-upwind schemes. In the remaining part of this section, we show the derivation of the second-order central-upwind scheme along the lines of Kurganov and Lin (2007).

The key idea is to select space–time control volumes in the finite-volume evolution procedure (3) adaptively depending on the size of Riemann fans generated at each cell interface. More precisely, we assume that, as before, the computed solution at time $t=t^n$ is available and realized in terms of the cell averages $\left\{\bar{\boldsymbol{q}}_j^{\,n}\right\}$ over the grid $\left[x_{j-\frac{1}{2}}, x_{j+\frac{1}{2}}\right]$. We first introduce the following notations:

$$\begin{aligned}\boldsymbol{q}_{j+\frac{1}{2}}^{n-} &:= \lim_{x\to x_{j+\frac{1}{2}}^-} \tilde{\boldsymbol{q}}^{\,n}(x) = \bar{\boldsymbol{q}}_j^{\,n} + \frac{\Delta x}{2}(\boldsymbol{q}_x)_j^n,\\ \boldsymbol{q}_{j+\frac{1}{2}}^{n+} &:= \lim_{x\to x_{j+\frac{1}{2}}^+} \tilde{\boldsymbol{q}}^{\,n}(x) = \bar{\boldsymbol{q}}_{j+1}^{\,n} - \frac{\Delta x}{2}(\boldsymbol{q}_x)_{j+1}^n\end{aligned} \tag{34}$$

for the reconstructed one-sided point values of $\boldsymbol{q}$ at the points $(x_{j+\frac{1}{2}}, t^n)$, and

$$\begin{aligned}a_{j+\frac{1}{2}}^{n+} &= \max\left\{\lambda_N\left(A\left(\boldsymbol{q}_{j+\frac{1}{2}}^{n+}\right)\right), \lambda_N\left(A\left(\boldsymbol{q}_{j+\frac{1}{2}}^{n-}\right)\right), 0\right\},\\ a_{j+\frac{1}{2}}^{n-} &= \min\left\{\lambda_1\left(A\left(\boldsymbol{q}_{j+\frac{1}{2}}^{n+}\right)\right), \lambda_1\left(A\left(\boldsymbol{q}_{j+\frac{1}{2}}^{n-}\right)\right), 0\right\}\end{aligned} \tag{35}$$

for the one-sided local speeds of propagation, which reduces to (19) in the case of the first-order piecewise constant reconstruction.

Remark 7. In fact, the estimate of one-sided local speed (35) is only true in the case of a convex flux $\boldsymbol{f}(\boldsymbol{q})$. In the nonconvex case, a more careful estimate is required; see Kurganov et al. (2007).

Remark 8. It might be impossible to exactly evaluate the largest and smallest eigenvalues of the Jacobian required in (35). In this case, one may use an upper bound on λ_N and a lower bound on λ_1 as it was done in, e.g., Kurganov and Petrova (2009) and Liu et al. (2015).

We then take the control volumes $\left[x_{j+\frac{1}{2},\ell}^n, x_{j+\frac{1}{2},r}^n\right] \times [t^n, t^{n+1}]$ that contain all of the waves generated at time $t = t^n$ at the corresponding cell interfaces

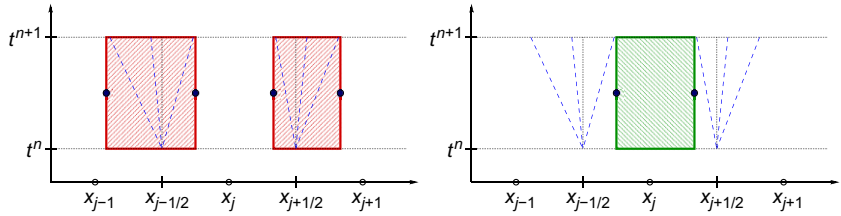

FIG. 4 Central-upwind control volumes over nonsmooth (*left*) and smooth (*right*) parts of the solution. *Dashed lines* represent Riemann fans generated at each cell interface at time $t = t^n$.

$x = x_{j+\frac{1}{2}}$; see Fig. 4 (left). The left and right boundaries of these control volumes, $x^n_{j+\frac{1}{2},\ell} := x_j + a^{n-}_{j+\frac{1}{2}}\Delta t^n$ and $x^n_{j+\frac{1}{2},r} := x_j + a^{n+}_{j+\frac{1}{2}}\Delta t^n$, respectively, are determined by the one-sided local speeds of propagation and therefore, the solution of the IVP (1) and (28) remains smooth at $x = x^n_{j+\frac{1}{2},\ell}$ and $x = x^n_{j+\frac{1}{2},r}$ for $t \in [t^n, t^{n+1}]$. Hence, the solution may be evolved to the time level $t = t^{n+1}$ exactly in the same manner as in the Nessyahu–Tadmor scheme, namely, we obtain the new cell averages, denoted by $\bar{\boldsymbol{q}}^{\,\text{int}}_{j+\frac{1}{2}}$, as follows. First, we use (3) to obtain

$$\bar{\boldsymbol{q}}^{\,\text{int}}_{j+\frac{1}{2}} = \frac{1}{x^n_{j+\frac{1}{2},r} - x^n_{j+\frac{1}{2},\ell}} \left\{ \int_{x^n_{j+\frac{1}{2},\ell}}^{x^n_{j+\frac{1}{2},r}} \tilde{\boldsymbol{q}}^{\,n}(x)\,dx - \int_{t^n}^{t^{n+1}} \left[\boldsymbol{f}\left(\boldsymbol{q}(x^n_{j+\frac{1}{2},r}, t)\right) - \boldsymbol{f}\left(\boldsymbol{q}(x^n_{j+\frac{1}{2},\ell}, t)\right) \right] dt \right\}. \tag{36}$$

Then, evaluating the first integral on the RHS of (36) exactly and using the midpoint rule for the flux integrals in (36), we arrive at

$$\bar{\boldsymbol{q}}^{\,\text{int}}_{j+\frac{1}{2}} = \frac{1}{a^{n+}_{j+\frac{1}{2}} - a^{n-}_{j+\frac{1}{2}}} \left\{ a^{n+}_{j+\frac{1}{2}} \boldsymbol{q}^{\,n}_{j+\frac{1}{2},r} - a^{n-}_{j+\frac{1}{2}} \boldsymbol{q}^{\,n}_{j+\frac{1}{2},\ell} + \frac{\Delta t^n}{2} \left[\left(a^{n-}_{j+\frac{1}{2}}\right)^2 (\boldsymbol{q}_x)^n_j - \left(a^{n+}_{j+\frac{1}{2}}\right)^2 (\boldsymbol{q}_x)^n_{j+1} \right] \right.$$
$$\left. - \left[\boldsymbol{f}\left(\boldsymbol{q}^{\,n+\frac{1}{2}}_{j+\frac{1}{2},r}\right) - \boldsymbol{f}\left(\boldsymbol{q}^{\,n+\frac{1}{2}}_{j+\frac{1}{2},\ell}\right) \right] \right\}, \tag{37}$$

where the point values of $\boldsymbol{q}$ at $\left(x^n_{j+\frac{1}{2},\ell}, t^n\right)$ and $\left(x^n_{j+\frac{1}{2},r}, t^n\right)$ are obtained from $\tilde{\boldsymbol{q}}^{\,n}(x)$:

$$\boldsymbol{q}^{\,n}_{j+\frac{1}{2},\ell} = \bar{\boldsymbol{q}}^{\,n}_j + \left(\frac{\Delta x}{2} + a^{n-}_{j+\frac{1}{2}}\Delta t^n\right)(\boldsymbol{q}_x)^n_j, \quad \boldsymbol{q}^{\,n}_{j+\frac{1}{2},r} = \bar{\boldsymbol{q}}^{\,n}_{j+1} - \left(\frac{\Delta x}{2} - a^{n+}_{j+\frac{1}{2}}\Delta t^n\right)(\boldsymbol{q}_x)^n_{j+1} \tag{38}$$

and the point values of $\boldsymbol{q}$ at $\left(x^n_{j+\frac{1}{2},\ell}, t^{n+\frac{1}{2}}\right)$ and $\left(x^n_{j+\frac{1}{2},r}, t^{n+\frac{1}{2}}\right)$ are predicted using the corresponding Taylor expansions:

$$\boldsymbol{q}^{\,n+\frac{1}{2}}_{j+\frac{1}{2},\ell} = \boldsymbol{q}^{\,n}_{j+\frac{1}{2},\ell} - \frac{\Delta t^n}{2}\boldsymbol{f}(\bar{\boldsymbol{q}}^{\,n}_j)_x, \quad \boldsymbol{q}^{\,n+\frac{1}{2}}_{j+\frac{1}{2},r} = \boldsymbol{q}^{\,n}_{j+\frac{1}{2},r} - \frac{\Delta t^n}{2}\boldsymbol{f}(\bar{\boldsymbol{q}}^{\,n}_{j+1})_x. \tag{39}$$

As one can see in Fig. 4 (left), even though the control volumes $\left[x^n_{j+\frac{1}{2},\ell}, x^n_{j+\frac{1}{2},r}\right] \times [t^n, t^{n+1}]$ contain all of the Riemann fans, they do not cover the entire strip $\mathbb{R} \times [t^n, t^{n+1}]$ since there are gaps between these control volumes, $\left[x^n_{j-\frac{1}{2},r}, x^n_{j+\frac{1}{2},\ell}\right] \times [t^n, t^{n+1}]$, shown in Fig. 4 (right), where the solution is smooth. The solution there is evolved using the same integral form (3), which results in

$$\bar{\boldsymbol{q}}_j^{\,\mathrm{int}} = \bar{\boldsymbol{q}}_j^{\,n} + \frac{\Delta t^n}{2}\left(a^{n+}_{j+\frac{1}{2}} + a^{n-}_{j+\frac{1}{2}}\right)(\boldsymbol{q}_x)^n_j - \frac{\Delta t^n}{\Delta x - \left(a^{n+}_{j+\frac{1}{2}} - a^{n-}_{j+\frac{1}{2}}\right)\Delta t^n}\left[\boldsymbol{f}\left(\boldsymbol{q}^{\,n+\frac{1}{2}}_{j+\frac{1}{2},\ell}\right) - \boldsymbol{f}\left(\boldsymbol{q}^{\,n+\frac{1}{2}}_{j-\frac{1}{2},r}\right)\right], \tag{40}$$

where the predicted values of $\boldsymbol{q}$ are, as before, given by (39).

At this stage, the approximate solution at time level $t = t^{n+1}$ is realized in terms of its cell averages $\left\{\bar{\boldsymbol{q}}^{\,\mathrm{int}}_{j+\frac{1}{2}}\right\}$ and $\left\{\bar{\boldsymbol{q}}^{\,\mathrm{int}}_{j}\right\}$, distributed over the nonuniform mesh $\bigcup_j\left\{\left[x^n_{j-\frac{1}{2},r}, x^n_{j+\frac{1}{2},\ell}\right] \cup \left[x^n_{j+\frac{1}{2},\ell}, x^n_{j+\frac{1}{2},r}\right]\right\}$. This solution is quite accurate, but impractical since the number of cells is doubled in just one time step, and this is the reason why it was denoted by $\boldsymbol{q}^{\mathrm{int}}$, where "int" stands for the intermediate. In order to complete construction of the central-upwind scheme, we need to project these intermediate data back onto the original grid $\bigcup_j C_j$. To this end, we use the intermediate data to reconstruct a conservative, non-oscillatory, second-order piecewise linear interpolant

$$\begin{aligned}\widetilde{\boldsymbol{q}}^{\,\mathrm{int}}(x) := \sum_j \Bigg\{ &\left[\bar{\boldsymbol{q}}^{\,\mathrm{int}}_{j+\frac{1}{2}} + (\boldsymbol{q}_x)^{\mathrm{int}}_{j+\frac{1}{2}}\left(x - \frac{x^n_{j+\frac{1}{2},\ell} + x^n_{j+\frac{1}{2},r}}{2}\right)\right]\chi_{\left[x^n_{j+\frac{1}{2},\ell},\, x^n_{j+\frac{1}{2},r}\right]} \\ &+ \left[\bar{\boldsymbol{q}}^{\,\mathrm{int}}_{j} + (\boldsymbol{q}_x)^{\mathrm{int}}_{j}\left(x - \frac{x^n_{j-\frac{1}{2},r} + x^n_{j+\frac{1}{2},\ell}}{2}\right)\right]\chi_{\left[x^n_{j-\frac{1}{2},r},\, x^n_{j+\frac{1}{2},\ell}\right]}\Bigg\},\end{aligned} \tag{41}$$

and average it over the cells C_j to end up with

$$\begin{aligned}\bar{\boldsymbol{q}}_j^{\,n+1} = {} & \lambda^n a^{n+}_{j-\frac{1}{2}}\bar{\boldsymbol{q}}^{\,\mathrm{int}}_{j-\frac{1}{2}} + \left[1 + \lambda^n\left(a^{n-}_{j-\frac{1}{2}} - a^{n+}_{j+\frac{1}{2}}\right)\right]\bar{\boldsymbol{q}}^{\,\mathrm{int}}_{j} \\ & - \lambda^n a^{n-}_{j+\frac{1}{2}}\bar{\boldsymbol{q}}^{\,\mathrm{int}}_{j+\frac{1}{2}} + \frac{\lambda^n \Delta t^n}{2}\left[a^{n+}_{j+\frac{1}{2}}a^{n-}_{j+\frac{1}{2}}(\boldsymbol{q}_x)^{\mathrm{int}}_{j+\frac{1}{2}} - a^{n+}_{j-\frac{1}{2}}a^{n-}_{j-\frac{1}{2}}(\boldsymbol{q}_x)^{\mathrm{int}}_{j-\frac{1}{2}}\right].\end{aligned} \tag{42}$$

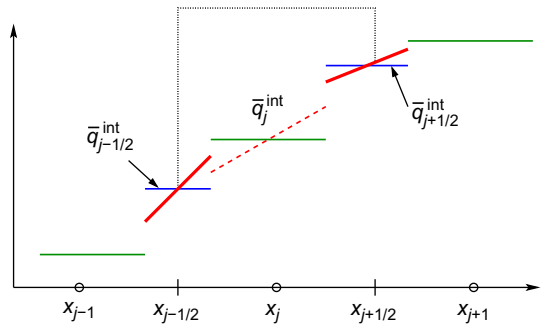

FIG. 5 Projection of the intermediate data onto the original grid.

In fact, we do not need to compute the slopes $(\boldsymbol{q}_x)^{\mathrm{int}}_j$ in (41) since they are "averaged out" at the averaging step (42); see Fig. 5. The slopes $(\boldsymbol{q}_x)^{\mathrm{int}}_{j+\frac{1}{2}}$ are to be computed using a nonlinear limiter. This may be done in several different ways. One of the sharpest possible approached, proposed in Kurganov and Lin (2007), uses the cell averages $\bar{\boldsymbol{q}}^{\,\mathrm{int}}_{j+\frac{1}{2}}$ and the predicted point values of $\boldsymbol{q}$ at time level $t = t^{n+1}$:

$$\boldsymbol{q}^{\,n+1}_{j+\frac{1}{2},\ell} = \boldsymbol{q}^{\,n}_{j+\frac{1}{2},\ell} - \Delta t^n \boldsymbol{f}(\bar{\boldsymbol{q}}^{\,n}_j)_x, \quad \boldsymbol{q}^{\,n+1}_{j+\frac{1}{2},r} = \boldsymbol{q}^{\,n}_{j+\frac{1}{2},r} - \Delta t^n \boldsymbol{f}(\bar{\boldsymbol{q}}^{\,n}_{j+1})_x \tag{43}$$

with $\boldsymbol{q}^{\,n}_{j+\frac{1}{2},\ell}$ and $\boldsymbol{q}^{\,n}_{j+\frac{1}{2},r}$ given by (38). The slopes are then obtained using the minmod limiter (see, e.g., Lie and Noelle, 2003; Nessyahu and Tadmor, 1990; Sweby, 1984; van Leer, 1979):

$$(\boldsymbol{q}_x)^{\mathrm{int}}_{j+\frac{1}{2}} = \mathrm{minmod}\left(\frac{\bar{\boldsymbol{q}}^{\,\mathrm{int}}_{j+\frac{1}{2}} - \boldsymbol{q}^{\,n+1}_{j+\frac{1}{2},\ell}}{\delta}, \frac{\boldsymbol{q}^{\,n+1}_{j+\frac{1}{2},r} - \bar{\boldsymbol{q}}^{\,\mathrm{int}}_{j+\frac{1}{2}}}{\delta}\right), \tag{44}$$

where $\delta = \left(x^n_{j+\frac{1}{2},r} - x^n_{j+\frac{1}{2},\ell}\right)/2 = \dfrac{\Delta t^n}{2}\left(a^{n+}_{j+\frac{1}{2}} - a^{n-}_{j+\frac{1}{2}}\right)$ and the minmod function, defined as

$$\mathrm{minmod}(a,b) = \frac{\mathrm{sign}(a) + \mathrm{sign}(b)}{2} \cdot \min\{|a|,|b|\},$$

is applied in (44) in a componentwise manner.

The resulting fully discrete central-upwind scheme (42), (37)–(40), (43), (44) is very accurate and robust and its numerical dissipation vanishes as $\max_n\{\Delta t^n\} \to 0$ (unlike the numerical dissipation of the Nessyahu–Tadmor and other staggered central schemes). This scheme has been tested on a number of numerical examples in Kurganov and Lin (2007); see also Kurganov et al. (2001); Kurganov and Tadmor (2000), where different, more dissipative versions of the fully discrete central-upwind schemes were derived and studied.

6.1 Semidiscrete Central-Upwind Schemes

A major disadvantage of the fully discrete central-upwind scheme (42), (37)–(40), (43), (44) is its relatively high complexity. This is especially pronounced when the scheme is extended to the two-dimensional (2D) case in a rigorous, genuinely multidimensional—not in a "dimension-by-dimension"—manner; see Kurganov and Lin (2007), Kurganov and Petrova (2001), Kurganov and Petrova (2005) and Kurganov et al. (2016). However, one may pass to a semidiscrete limit as $\max_n\{\Delta t^n\}\to 0$ and derive semidiscrete central-upwind schemes, which are substantially simpler than their fully discrete counterparts and yet accurate and robust.

In order to derive a semidiscrete central-upwind scheme, we need to compute the following limit:

$$\frac{d}{dt}\bar{\boldsymbol{q}}_j(t^n)=\lim_{\Delta t^n\to 0}\frac{\bar{\boldsymbol{q}}_j^{\,n+1}-\bar{\boldsymbol{q}}_j^{\,n}}{\Delta t^n}. \tag{45}$$

After substituting (42) and then (37)–(40), (43) and (44) into (45) (see details in Kurganov and Lin (2007) and also in Kurganov et al. (2001), Kurganov and Petrova (2000) and Kurganov and Tadmor (2000)), we arrive at a particularly simple semidiscrete scheme, which can be written in the flux form as follows:

$$\frac{d}{dt}\bar{\boldsymbol{q}}_j(t)=-\frac{\boldsymbol{H}_{j+\frac12}(t)-\boldsymbol{H}_{j-\frac12}(t)}{\Delta x} \tag{46}$$

with the numerical fluxes

$$\boldsymbol{H}_{j+\frac12}(t)=\frac{a^+_{j+\frac12}\boldsymbol{f}\left(\boldsymbol{q}^-_{j+\frac12}\right)-a^-_{j+\frac12}\boldsymbol{f}\left(\boldsymbol{q}^+_{j+\frac12}\right)}{a^+_{j+\frac12}-a^-_{j+\frac12}}+a^+_{j+\frac12}a^-_{j+\frac12}\left[\frac{\boldsymbol{q}^+_{j+\frac12}-\boldsymbol{q}^-_{j+\frac12}}{a^+_{j+\frac12}-a^-_{j+\frac12}}-\boldsymbol{d}_{j+\frac12}\right], \tag{47}$$

where

$$\boldsymbol{d}_{j+\frac12}=\frac12\lim_{\Delta t^n\to 0}\left\{\Delta t^n(\boldsymbol{q}_x)^{\text{int}}_{j+\frac12}\right\}=\text{minmod}\left(\frac{\boldsymbol{q}^+_{j+\frac12}-\boldsymbol{q}^*_{j+\frac12}}{a^+_{j+\frac12}-a^-_{j+\frac12}},\frac{\boldsymbol{q}^*_{j+\frac12}-\boldsymbol{q}^-_{j+\frac12}}{a^+_{j+\frac12}-a^-_{j+\frac12}}\right) \tag{48}$$

is a built-in "anti-diffusion" term and

$$\boldsymbol{q}^*_{j+\frac12}=\lim_{\Delta t^n\to 0}\bar{\boldsymbol{q}}^{\,\text{int}}_{j+\frac12}=\frac{a^+_{j+\frac12}\boldsymbol{q}^+_{j+\frac12}-a^-_{j+\frac12}\boldsymbol{q}^-_{j+\frac12}-\left\{\boldsymbol{f}(\boldsymbol{q}^+_{j+\frac12})-\boldsymbol{f}(\boldsymbol{q}^-_{j+\frac12})\right\}}{a^+_{j+\frac12}-a^-_{j+\frac12}} \tag{49}$$

In (47)–(49), the reconstructed point values $\boldsymbol{q}^{\pm}_{j+\frac12}$ and the local one-sided speeds of propagation $a^{\pm}_{j+\frac12}$ are given by (34) and (35), respectively, but

without the upper index n, since these quantities are now computed at some time level t rather than t^n. Note that all of the terms on the RHS of (47) and in (48) and (49) depend on t, but we omit this dependence for the sake of brevity.

Remark 9. The semidiscretization (46)–(49) results in a system of time-dependent ODEs, which should be integrated using a sufficiently accurate and stable ODE solver. In the purely convective and convective-dominated cases, the ODE system is nonstiff and we usually solve it using the three-stage third-order strong stability preserving Runge-Kutta method; see Gottlieb et al. (2011, 2001).

Remark 10. Both the fully and semidiscrete central-upwind schemes belong to the class of Godunov-type Riemann-problem-solver-free central schemes, but since they are constructed using some upwind information (one-sided local speeds), we call them central-upwind schemes.

Remark 11. In the older works on central-upwind schemes (Kurganov et al., 2001; Kurganov and Petrova, 2000, 2001; Kurganov and Tadmor, 2000, 2002), the slopes $(\boldsymbol{q}_x)^{\text{int}}_{j+\frac{1}{2}}$ in (42) were not computed in a sharp way (formula (44) was only proposed in Kurganov and Lin (2007)) and therefore, the built-in anti-diffusion term $\boldsymbol{d}_{j+\frac{1}{2}}$ in (47) was equal to zero.

Remark 12. The first central-upwind scheme, introduced in Kurganov and Tadmor (2000), was obtained by setting the symmetric bounds on the local speeds, namely, by replacing (35) with

$$a^{n\pm}_{j+\frac{1}{2}} = \pm\max\left\{\rho\left(A\left(\bar{\boldsymbol{q}}^{\,n+}_{j+\frac{1}{2}}\right)\right), \rho\left(A\left(\bar{\boldsymbol{q}}^{\,n-}_{j+\frac{1}{2}}\right)\right)\right\}. \tag{50}$$

Remark 13. If the piecewise constant reconstruction (7) and the forward Euler ODE solver are used, the central-upwind schemes from Kurganov and Petrova (2001) and Kurganov and Tadmor (2000) reduce to the first-order Rusanov scheme (11), (16) and (17), while the central-upwind schemes from Kurganov et al. (2001), Kurganov and Petrova (2000) and Kurganov and Tadmor (2002) reduce to the first-order HLL scheme (11), (18) and (19).

Remark 14. If the point values $\left\{\boldsymbol{q}^{\pm}_{j+\frac{1}{2}}\right\}$ are computed using a reconstruction of order r (see Section 5.3), then the semidiscrete central-upwind scheme (46)–(49) will be (formally) rth order accurate.

Remark 15. Semidiscrete central-upwind schemes have been rigorously (using a genuinely multidimensional approach) extended to general 2D hyperbolic systems on a variety of different grids. We refer the reader to Kurganov and Lin (2007), Kurganov et al. (2001), Kurganov and Petrova (2001) and Kurganov and Tadmor (2002) for the central-upwind schemes on the Cartesian meshes. Triangular version of the central-upwind scheme was derived in Kurganov and Petrova (2005). Central-upwind scheme on general quadrilateral

grids was introduced in Shirkhani et al. (2016) (see also Kurganov et al. (2016)). Finally, central-upwind schemes on cell-vertex polygonal meshes was developed in Beljadid et al. (2016).

Remark 16. When semidiscrete central-upwind schemes are applied to systems of balance laws

$$\boldsymbol{q}_t + \boldsymbol{f}(\boldsymbol{q})_x = \boldsymbol{S}(x,t,\boldsymbol{q}), \tag{51}$$

the numerical fluxes are still given by (47)–(49) and the only degree of freedom is in the approximation of cell averages of the source term, $\frac{1}{\Delta x}\int_{C_j} \boldsymbol{S}(x,t,\boldsymbol{q})\,dx$, which has to be added to the RHS of (46). In order to construct a reliable and robust method, one has to carefully choose an appropriate quadrature, which respects a delicates balance between the flux and source terms in (51). For instance, semidiscrete central-upwind schemes have been applied to a variety of shallow water models with the source terms describing the bottom topography, friction, and Coriolis forces. Well-balanced central-upwind schemes were developed in, e.g., Beljadid et al. (2016), Bryson et al. (2011), Cheng and Kurganov (2016), Chertock et al. (2015), Chertock et al. (2016), Kurganov and Levy (2002), Kurganov and Petrova (2007) and Shirkhani et al. (2016).

ACKNOWLEDGEMENTS

The author was supported in part by the NSF Grants DMS-1216957 and DMS-1521009.

REFERENCES

Abgrall, R., 1994. On essentially non-oscillatory schemes on unstructured meshes: analysis and implementation. J. Comput. Phys. 114, 45–58.

Arminjon, P., Viallon, M.-C., Madrane, A., 1997. A finite volume extension of the Lax-Friedrichs and Nessyahu-Tadmor schemes for conservation laws on unstructured grids. Int. J. Comput. Fluid Dyn. 9, 1–22.

Beljadid, A., Mohammadian, A., Kurganov, A., 2016. Well-balanced positivity preserving cell-vertex central-upwind scheme for shallow water flows. Comput. Fluids 136, 193–206.

Ben-Artzi, M., Falcovitz, J., 2003. Generalized Riemann Problems in Computational Fluid Dynamics, Cambridge Monographs on Applied and Computational Mathematics, vol. 11. Cambridge University Press, Cambridge, xvi+349. ISBN 0-521-77296-6.

Bianco, F., Puppo, G., Russo, G., 1999. High order central schemes for hyperbolic systems of conservation laws. SIAM J. Sci. Comput 21, 294–322.

Bryson, S., Epshteyn, Y., Kurganov, A., Petrova, G., 2011. Well-balanced positivity preserving central-upwind scheme on triangular grids for the Saint-Venant system. M2AN Math. Model. Numer. Anal. 45 (3), 423–446.

Buffard, T., Gallouët, T., Hérard, J.-M., 2000. A sequel to a rough Godunov scheme: application to real gases. Comput. Fluids 29 (7), 813–847.

Caramana, E.J., Shashkov, M.J., Whalen, P.P., 1998. Formulations of artificial viscosity for multi-dimensional shock wave computations. J. Comput. Phys. 144 (1), 70–97.

Cheng, Y., Kurganov, A., 2016. Moving-water equilibria preserving central-upwind schemes for the shallow water equations. Commun. Math. Sci. 14 (6), 1643–1663.

Chertock, A., Cui, S., Kurganov, A., Wu, T., 2015. Well-balanced positivity preserving central-upwind scheme for the shallow water system with friction terms. Int. J. Numer. Meth. Fluids 78, 355–383.

Chertock, A., Dudzinski, M., Kurganov, A., Lukáčová-Medviďová, M., 2016. Well-balanced schemes for the shallow water equations with Coriolis forces (submitted for publication).

Cockburn, B., Johnson, C., Shu, C.-W., Tadmor, E., 1998. Advanced numerical approximation of nonlinear hyperbolic equations. In: Quarteroni, A. (Ed.), CIME Lecture Notes. Lecture Notes in Mathematics, vol. 1697. Springer-Verlag, Berlin, Heidelberg.

Dafermos, C.M., 2010. Hyperbolic Conservation Laws in Continuum Physics, third ed. Grundlehren der Mathematischen Wissenschaften [Fundamental Principles of Mathematical Sciences], vol. 325. Springer-Verlag, Berlin, xxxvi+708.

Einfeld, B., 1988. On Godunov-type methods for gas dynamics. SIAM J. Numer. Anal. 25, 294–318.

Friedrichs, K.O., 1954. Symmetric hyperbolic linear differential equations. Comm. Pure Appl. Math. 7, 345–392.

Gallouët, T., Hérard, J.-M., Seguin, N., 2002. Some recent finite volume schemes to compute Euler equations using real gas EOS. Int. J. Numer. Methods Fluids 39 (12), 1073–1138.

Godlewski, E., Raviart, P.-A., 1996. Numerical Approximation of Hyperbolic Systems of Conservation Laws. Applied Mathematical Sciences, vol. 118. Springer-Verlag, New York, viii+509.

Godunov, S.K., 1959. A difference method for numerical calculation of discontinuous solutions of the equations of hydrodynamics. Mat. Sb. (N.S.) 47 (89), 271–306.

Gottlieb, S., Shu, C.-W., Tadmor, E., 2001. Strong stability-preserving high-order time discretization methods. SIAM Rev. 43, 89–112.

Gottlieb, S., Ketcheson, D., Shu, C.-W., 2011. Strong Stability Preserving Runge-Kutta and Multistep Time Discretizations. World Scientific Publishing Co. Pte. Ltd., Hackensack, NJ, xii+176.

Guermond, J.-L., Pasquetti, R., 2008. Entropy-based nonlinear viscosity for Fourier approximations of conservation laws. C. R. Math. Acad. Sci. Paris 346 (13–14), 801–806.

Guermond, J.-L., Pasquetti, R., Popov, B., 2011. Entropy viscosity method for nonlinear conservation laws. J. Comput. Phys. 230 (11), 4248–4267.

Harten, A., Lax, P., van Leer, B., 1983. On upstream differencing and Godunov-type schemes for hyperbolic conservation laws. SIAM Rev. 25, 35–61.

Harten, A., Engquist, B., Osher, S., Chakravarthy, S.R., 1987. Uniformly high-order accurate essentially nonoscillatory schemes. III. J. Comput. Phys. 71 (2), 231–303.

Jiang, G.-S., Shu, C.-W., 1996. Efficient implementation of weighted ENO schemes. J. Comput. Phys. 126 (1), 202–228.

Jiang, G.-S., Tadmor, E., 1998. Nonoscillatory central schemes for multidimensional hyperbolic conservation laws. SIAM J. Sci. Comput. 19 (6), 1892–1917. (electronic).

Kröner, D., 1997. Numerical Schemes for Conservation Laws. Wiley-Teubner Series Advances in Numerical Mathematics. John Wiley & Sons Ltd., Chichester, viii+508.

Kurganov, A., Levy, D., 2002. Central-upwind schemes for the Saint-Venant system. M2AN Math. Model. Numer. Anal. 36, 397–425.

Kurganov, A., Lin, C.T., 2007. On the reduction of numerical dissipation in central-upwind schemes. Commun. Comput. Phys. 2, 141–163.

Kurganov, A., Liu, Y., 2012. New adaptive artificial viscosity method for hyperbolic systems of conservation laws. J. Comput. Phys. 231, 8114–8132.

Kurganov, A., Petrova, G., 2000. Central schemes and contact discontinuities. M2AN Math. Model. Numer. Anal. 34 (6), 1259–1275.

Kurganov, A., Petrova, G., 2001. A third-order semi-discrete genuinely multidimensional central scheme for hyperbolic conservation laws and related problems. Numer. Math. 88 (4), 683–729.

Kurganov, A., Petrova, G., 2005. Central-upwind schemes on triangular grids for hyperbolic systems of conservation laws. Numer. Methods Partial Differ. Equ. 21, 536–552.

Kurganov, A., Petrova, G., 2007. A second-order well-balanced positivity preserving central-upwind scheme for the Saint-Venant system. Commun. Math. Sci. 5, 133–160.

Kurganov, A., Petrova, G., 2009. Central-upwind schemes for two-layer shallow equations. SIAM J. Sci. Comput. 31, 1742–1773.

Kurganov, A., Tadmor, E., 2000. New high resolution central schemes for nonlinear conservation laws and convection-diffusion equations. J. Comput. Phys. 160, 241–282.

Kurganov, A., Tadmor, E., 2002. Solution of two-dimensional Riemann problems for gas dynamics without Riemann problem solvers. Numer. Methods Partial Differ. Equ. 18, 584–608.

Kurganov, A., Noelle, S., Petrova, G., 2001. Semi-discrete central-upwind scheme for hyperbolic conservation laws and Hamilton-Jacobi equations. SIAM J. Sci. Comput. 23, 707–740.

Kurganov, A., Petrova, G., Popov, B., 2007. Adaptive semi-discrete central-upwind schemes for nonconvex hyperbolic conservation laws. SIAM J. Sci. Comput. 29, 2381–2401.

Kurganov, A., Prugger, M., Wu, T., 2016. Second-order fully discrete central-upwind scheme for two-dimensional hyperbolic systems of conservation laws (submitted for publication).

Lax, P.D., 1954. Weak solutions of nonlinear hyperbolic equations and their numerical computation. Comm. Pure Appl. Math. 7, 159–193.

LeFloch, P.G., 2002. Hyperbolic Systems of Conservation Laws. Lectures in Mathematics ETH Zürich. Birkhäuser Verlag, Basel. x+294.

LeVeque, R.J., 2002. Finite Volume Methods for Hyperbolic Problems. Cambridge texts in applied mathematics. Cambridge University Press, Cambridge, pp. xx+558.

Levy, D., Puppo, G., Russo, G., 1999. Central WENO schemes for hyperbolic systems of conservation laws. M2AN Math. Model. Numer. Anal. 33 (3), pp. 547–571.

Levy, D., Puppo, G., Russo, G., 2000. Compact central WENO schemes for multidimensional conservation laws. SIAM J. Sci. Comput. 22 (2), 656–672. (electronic).

Levy, D., Puppo, G., Russo, G., 2002. A fourth-order central WENO scheme for multidimensional hyperbolic systems of conservation laws. SIAM J. Sci. Comput. 24 (2), 480–506.

Li, J., Zhang, T., Yang, S., 1998. The Two-dimensional Riemann Problem in Gas Dynamics. Pitman Monographs and Surveys in Pure and Applied Mathematics, vol. 98. Longman, Harlow. x+300. 0-8493-0693-0.

Lie, K.A., Noelle, S., 2003. On the artificial compression method for second-order nonoscillatory central difference schemes for systems of conservation laws. SIAM J. Sci. Comput. 24 (4), 1157–1174.

Liu, Y., 2005. Central schemes on overlapping cells. J. Comput. Phys. 209 (1), 82–104.

Liu, X.D., Osher, S., 1996. Nonoscillatory high order accurate self-similar maximum principle satisfying shock capturing schemes. I. SIAM J. Numer. Anal. 33 (2), 760–779.

Liu, X.D., Tadmor, E., 1998. Third order nonoscillatory central scheme for hyperbolic conservation laws. Numer. Math. 79 (3), 397–425.

Liu, Y., Shu, C.-W., Tadmor, E., Zhang, M., 2007. Non-oscillatory hierarchical reconstruction for central and finite volume schemes. Commun. Comput. Phys. 2 (5), 933–963.

Liu, Y., Shu, C.-W., Xu, Z., 2009. Hierarchical reconstruction with up to second degree remainder for solving nonlinear conservation laws. Nonlinearity 22 (12), 2799–2812.

Liu, X., Mohammadian, A., Kurganov, A., Infante Sedano, J.A., 2015. Well-balanced central scheme for a fully coupled shallow water system modeling flows over erodible bed. J. Comput. Phys. 300, 202–218.

Masella, J.M., Faille, I., Gallouët, T., 1999. On an approximate Godunov scheme. Int. J. Comput. Fluid Dyn. 12 (2), 133–149.

Nessyahu, H., Tadmor, E., 1990. Nonoscillatory central differencing for hyperbolic conservation laws. J. Comput. Phys. 87 (2), 408–463.

Qiu, J., Shu, C.-W., 2002. On the construction, comparison, and local characteristic decomposition for high-order central WENO schemes. J. Comput. Phys. 183 (1), 187–209.

Roe, P.L., 1981. Approximate Riemann solvers, parameter vectors, and difference schemes. J. Comput. Phys. 43 (2), 357–372.

Rusanov, V.V., 1961. The calculation of the interaction of non-stationary shock waves with barriers. Zh. Vychisl. Mat. Mat. Fiz. 1, 267–279.

Serre, D., 1999. Systems of Conservation Laws. 1. Cambridge University Press, Cambridge, xxii+263.

Shchepetkin, A.F., McWilliams, J.C., 1998. Quasi-monotone advection schemes based on explicit locally adaptive dissipation. Mon. Weather Rev. 126, 1541–1580.

Shi, J., Hu, C., Shu, C.-W., 2002. A technique of treating negative weights in weno schemes. J. Comput. Phys. 175 (1), 108–127.

Shirkhani, H., Mohammadian, A., Seidou, O., Kurganov, A., 2016. A well-balanced positivity-preserving central-upwind scheme for shallow water equations on unstructured quadrilateral grids. Comput. Fluids 126, 25–40.

Shu, C.-W., 2003. High-order finite difference and finite volume WENO schemes and discontinuous Galerkin methods for CFD. Int. J. Comput. Fluid Dyn. 17 (2), 107–118.

Shu, C.-W., 2009. High order weighted essentially nonoscillatory schemes for convection dominated problems. SIAM Rev. 51 (1), 82–126.

Smoller, J., 1994. Shock Waves and Reaction-Diffusion Equations, second ed. Grundlehren der Mathematischen Wissenschaften [Fundamental Principles of Mathematical Sciences], vol. 258. Springer-Verlag, New York, xxiv–632.

Sweby, P.K., 1984. High resolution schemes using flux limiters for hyperbolic conservation laws. SIAM J. Numer. Anal. 21 (5), 995–1011.

Tadmor, E., 1984a. The large-time behavior of the scalar, genuinely nonlinear Lax-Friedrichs scheme. Math. Comp. 43 (168), 353–368.

Tadmor, E., 1984b. Numerical viscosity and the entropy condition for conservative difference schemes. Math. Comp. 43 (168), 369–381.

Toro, E.F., 2009. Riemann Solvers and Numerical Methods for Fluid Dynamics: A Practical Introduction, third ed. Springer-Verlag, Berlin, Heidelberg, xx+724.

Toro, E.F., Spruce, M., Speares, W., 1994. Restoration of the contact surface in the HLL-Riemann solver. Shock Waves 4 (1), 25–34.

van Leer, B., 1979. Towards the ultimate conservative difference scheme. V. A second-order sequel to Godunov's method. J. Comput. Phys. 32 (1), 101–136.

von Neumann, J., Richtmyer, R.D., 1950. A method for the numerical calculation of hydrodynamic shocks. J. Appl. Phys. 21, 232–237.

Wilkins, M.L., 1980. Use of artificial viscosity in multidimensional fluid dynamic calculations. J. Comput. Phys. 36, 281–303.

Yang, S., Kurganov, A., Liu, Y., 2015. Well-balanced central schemes on overlapping cells with constant subtraction techniques for the Saint-Venant shallow water system. J. Sci. Comput. 63 (3), 678–698.

Zheng, Y., 2001. Systems of Conservation Laws, Progress in Nonlinear Differential Equations and their Applications, 38, Birkhäuser Boston, Inc., Boston, MA. xvi+317. ISBN 0-8176-4080-0.